CONTROL OF SEISMIC-EXCITED NONLINEAR ISOLATED BRIDGES WITH VARIABLE VISCOUS DAMPERS

Tzu-Ying LEE[1] and Kazuhiko KAWASHIMA[2]

[1] Graduate Student, Department of Civil Engineering, Tokyo Institute of Technology
Tokyo 152-8552, Japan, tylee@cv.titech.ac.jp
[2] Professor, Department of Civil Engineering, Tokyo Institute of Technology
Tokyo 152-8552, Japan, kawasima@ cv.titech.ac.jp

The application and effectiveness of seismic response control with variable viscous dampers for nonlinear isolated bridges is studied. Upon considering practical applications, the LQR optimal control algorithm is used to command variable viscous dampers. A typical viaduct is analyzed for evaluation. Through numerical simulation, the results show that the semi-active control system with variable dampers is effective for reducing the seismic displacement response and provides the similar performance by LQR active control with actuators.

Key words: *Nonlinear isolated bridge, seismic response, variable viscous damper, semi-active control*

1. INTRODUCTION

The isolator in bridge structure is effective to mitigate the induced seismic force by a shift of natural period. However, the deck displacement becomes excessively large when subjected to a ground motion with large intensity or unexpected characteristics. Even in a standard-size bridge a deck displacement reaches 0.5m or larger under the ground motions developed in the 1999 Chi-Chi earthquake. Such a large displacement may result in the higher-than-expected seismic force due to the pounding effect of decks and the $P-\delta$ effects[1]. In the previous studies[2-5], structural controls were studied to effectively reducing seismic responses of isolated bridges. However, the control effectiveness of the isolated bridges, which exhibit high hysteretic behavior at both the column and the isolator has not yet been reported. Hence it is emphasized in this study to reduce the deck displacement of isolated bridges with nonlinearity of both the column and the isolator using seismic response control technology.
Although active control systems have been studied to effectively mitigate the seismic response of structures, they require large external power supply and their reliability is still the issue of concern. Semi-active control systems have the major advantages of the versatility and adaptability of active control systems without large energy supply, and have the reliability of passive control systems. One means of achieving a semi-active control is to adopt a variable viscous damper, in which the damping coefficient can be regulated. Variable viscous dampers have been studied analytically and experimentally to effectively mitigate seismic response of bridges and buildings (Kawashima et al.[2], Yang et al.[3], Symans and Constantinou[6]).
This study focuses on the application of variable viscous dampers to reduce the seismic response of nonlinear isolated bridges. The recent control theories for nonlinear system were proposed by Yang et al.[7,8]. Upon considering practical applications, the linear quadratic regulator (LQR) optimal control algorithm is used here to command variable viscous dampers. A five-span viaduct with high-damping-rubber isolators, designed based on Japan Design Specification of Highway Bridges, is utilized for analysis.

2. ANALYSIS MODEL FOR NONLINEAR ISOLATED BRIDGE

Assuming the deck of a typical isolated bridge is rigid in the longitudinal direction, a column with the effective deck mass on the top can be taken apart as a unit for seismic analysis, as shown in Fig. 1. For study of control effectiveness, the column-deck-isolator system may be idealized as a two degree of freedom lumped-mass system. A control device is set between the deck and the column where the isolators are installed.

The column and the isolator are assumed here to be perfect elastoplastic and bilinear elastoplastic, respectively. The Bouc-Wen hysteretic model[9] is used for the column and the isolator as

$$F_{si}(t) = \alpha_i k_i x_i(t) + (1-\alpha_i) k_i x_{yi} v_i(t) \quad (i = c \text{ and } b) \tag{1}$$

in which the subscripts c and b denote the column and the isolator, respectively, e.g. x_c = deformation of the column and x_b = deformation of the isolator; k_i = initial stiffness; α_i = ratio of the post-yielding to pre-yielding stiffness; x_{yi} = yield deformation; and v_i is a nondimensional variable introduced to describe the hysteretic component of the deformation with $|v_i| \le 1$, where

$$\dot{v}_i = x_{yi}^{-1}\left[A_i \dot{x}_i - \beta_i |\dot{x}_i| |v_i|^{n_i - 1} v_i - \gamma_i \dot{x} |v|^{n_i}\right] \tag{2}$$

in which parameters A_i, β_i and γ_i govern the scale and general shape of hysteresis loop, whereas the smoothness of force-deformation curve is determined by the parameter n_i. These parameters are considered time invariant herein.

The equations of motion of the isolated bridge system may be expressed as

$$\mathbf{M}\ddot{\mathbf{x}}(t) + \mathbf{C}\dot{\mathbf{x}}(t) + \mathbf{K}_e \mathbf{x}(t) + \mathbf{K}_I \mathbf{v}(t) = \boldsymbol{\eta}\ddot{x}_g(t) + \mathbf{H}U(t) \tag{3}$$

in which $\mathbf{x} = \begin{bmatrix} x_c & x_b \end{bmatrix}^T$ is a vector with the deformations of the column and the isolator; $\mathbf{v} = \begin{bmatrix} v_c & v_b \end{bmatrix}^T$ is a hysteretic vector; $\ddot{x}_g(t)$ is the absolute ground acceleration; $U(t)$ is the control force generated by the control device; $\mathbf{M}$, $\mathbf{C}$, $\mathbf{K}_e$ and $\mathbf{K}_I$ are mass, damping, elastic stiffness and hysteretic stiffness matrices, respectively; $\boldsymbol{\eta}$ and $\mathbf{H}$ are the location matrices of the excitation and the control force, respectively. These matrices are given by

$$\mathbf{M} = \begin{bmatrix} m_c & 0 \\ m_d & m_d \end{bmatrix}; \quad \mathbf{C} = \begin{bmatrix} c_c & -c_b \\ 0 & c_b \end{bmatrix};$$

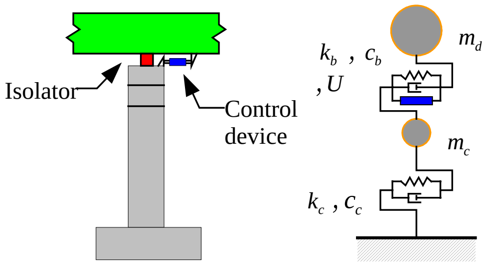

Figure 1 Analytical idealization

$$\mathbf{K}_e = \begin{bmatrix} \alpha_c k_c & -\alpha_b k_b \\ 0 & \alpha_b k_b \end{bmatrix};$$

$$\mathbf{K}_I = \begin{bmatrix} (1-\alpha_c) k_c x_{yc} & -(1-\alpha_b) k_b x_{yb} \\ 0 & (1-\alpha_b) k_b x_{yb} \end{bmatrix};$$

$$\boldsymbol{\eta} = \begin{bmatrix} -m_d \\ -m_c \end{bmatrix}; \quad \mathbf{H} = \begin{bmatrix} 1 \\ -1 \end{bmatrix} \tag{4}$$

where m_c and m_d are the masses of the column and the deck, respectively; c_c and c_d are the damping coefficients of the column and the isolator, respectively.

The equations of motion by Equation (3) can be written as a state space formulation as

$$\dot{\mathbf{Z}}(t) = \mathbf{g}[\mathbf{Z}(t), \mathbf{v}(t)] + \mathbf{B}U(t) + \mathbf{W}\ddot{x}_g(t) \tag{5}$$

where $\mathbf{Z}(t) = \begin{bmatrix} \mathbf{x}(t) & \dot{\mathbf{x}}(t) \end{bmatrix}^T$ is a space-state vector; $\mathbf{g}\left[\mathbf{Z}(t), \mathbf{v}(t)\right]$ is a nonlinear function of $\mathbf{Z}(t)$ and $\mathbf{v}(t)$; $\mathbf{B}$ and $\mathbf{W}$ are the matrices of the control location and the excitation location, respectively. $\mathbf{g}$, $\mathbf{B}$ and $\mathbf{W}$ are defined as follows:

$$\mathbf{g}[\mathbf{Z}(t)] = \begin{bmatrix} \dot{\mathbf{x}} \\ -\mathbf{M}^{-1}[\mathbf{C}\dot{\mathbf{x}} + \mathbf{K}_e \mathbf{x} + \mathbf{K}_I \mathbf{v}] \end{bmatrix};$$

$$\mathbf{B} = \begin{bmatrix} 0 \\ \mathbf{M}^{-1}\mathbf{H} \end{bmatrix}; \quad \mathbf{W} = \begin{bmatrix} 0 \\ \mathbf{M}^{-1}\boldsymbol{\eta} \end{bmatrix} \tag{6}$$

3. CONTROL ALGORITHM

The linear quadratic regulator (LQR) optimal control algorithm has been extensively used for active control and for semi-active control of structures (e.g. Soong[10], Symans and Constantinou[6]). In this algorithm, the control force $U(t)$ in Equation (3) is selected by minimizing, over the duration of the excitation, the quadratic cost function

$$J = \int_0^{t_f} [\mathbf{Z}^T(t)\mathbf{Q}\mathbf{Z}(t) + RU^2(t)]dt \tag{7}$$

in which $\mathbf{Q}$ is a (4 × 4) symmetric positive semidefinite weighting matrix and R is a positive weighting scalar. The weighting values should be determined depending on the design performance goals and the constraints on the controller.

The optimal solution that minimizes the performance index, as shown in Equation (7), is obtained under the constraint of the state equations of motion by Equation (5) as [7)]

$$U(t) = -0.5R^{-1}\mathbf{B}^T\mathbf{PZ}(t) \tag{8}$$

in which $\mathbf{P}$ is the solution of Ricatti equation given by

$$\mathbf{\Lambda_0}'\mathbf{P} + \mathbf{P\Lambda_0} - 0.5\mathbf{PB}R^{-1}\mathbf{B}^T\mathbf{P} = -2\mathbf{Q} \tag{9}$$

where

$$\mathbf{\Lambda_0} = \partial\mathbf{g}(\mathbf{Z})/\partial\mathbf{Z}|_{\mathbf{Z}=0} \tag{10}$$

Note that the constant Ricatti matrix $\mathbf{P}$ in Equation (9) is obtained by linearizing the structure at the initial equilibrium point $\mathbf{Z}=0$, which is stable, as shown in Equation (10), neglecting the ground excitation $\ddot{x}_g(t)$ and setting the transient part equal to zero, i.e. $\dot{\mathbf{P}}=0$.

When a variable viscous damper is used as the control device, which is referred hereinafter to semi-active control, the control force $V(t)$ from the variable viscous damper is given by

$$V(t) = \xi_b(t)\dot{x}_b(t) \tag{11}$$

where $\xi_b(t)$ is the time-variant damping coefficient and $\dot{x}_b(t)$ is the relative velocity of the isolator.

It is noted that the control force cannot be commanded directly but viscous coefficient has to be regulated in the variable viscous damper. The damping coefficient is bounded by a minimum value $\xi_{\min}$ and a maximum value $\xi_{\max}$ as

$$\xi_{\min} \le \xi_b(t) \le \xi_{\max} \tag{12}$$

When the variable viscous damper is expected to provide the desired optimal control force $U(t)$ by Equation (8), equaling Equation (11) and Equation (8) leads to

$$\xi_b^*(t)\dot{x}_b(t) = U(t) = -0.5R^{-1}\mathbf{B}^T\mathbf{PZ}(t) \tag{13}$$

By dividing Equation (13) by $\dot{x}_b(t)$, the demanded active damping coefficient $\xi_b^*(t)$ is

$$\xi_b^*(t) = \frac{U(t)}{\dot{x}_b(t)} \tag{14}$$

Note that the viscous damping coefficient $\xi_b(t)$ has the following constrain from Equation (12)

$$\xi_b(t) = \begin{cases} \xi_{\max} & \xi_b^* \ge \xi_{\max} \\ \xi_b^* & \xi_{\min} < \xi_b^* < \xi_{\max} \\ \xi_{\min} & \xi_b^* \le \xi_{\min} \end{cases} \tag{15}$$

Therefore, the variable viscous damper not only changes the damping coefficient depending on feedback of structural responses to resemble an active system but also functions as a passive energy dissipater.

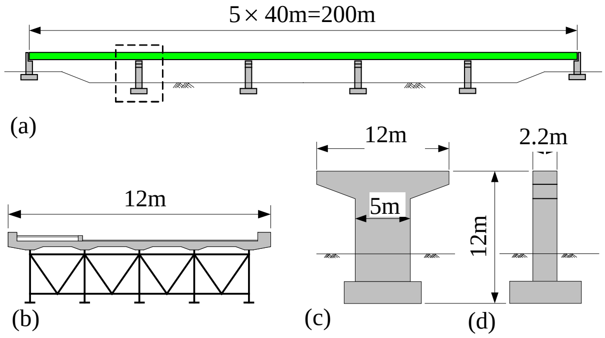

Figure 2 A continuous elevated highway bridge (a) elevation, (b) lateral view of superstructure, (c) lateral view of column, and (d) side view of column.

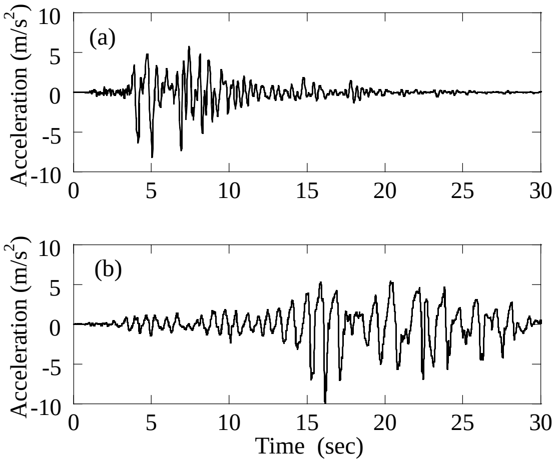

Figure 3 Ground motion records: (a) JMA Kobe observatory, and (b) Sun-Moon Lake

4. NUMERICAL SIMULATION

(1) Target viaduct

In this study, an isolated bridge as shown in Fig. 2, which was designed by Japan Design Specification of Highway Bridges[10)], was analyzed to investigate the performance of structural control. The superstructure consists of a five-span continuous deck with a total deck length of 5@40 m = 200 m and a width of 12 m. They are supported by 12 m tall reinforced concrete columns. Five high-damping-rubber isolators with 112 mm × 600 mm × 600 mm ($H \times B \times D$) are used per column.

The bridge is idealized as a two degree of freedom lumped-mass system. The effective mass of deck and column are 600 T and 243.15 T, respectively. As described earlier, the restoring forces of the

Table 1 Summary of peak control force and peak responses under JMA Kobe record

Peak force (KN) and responses (m) (1)	Uncontrolled (2)	Active I $R=10^{-11}$ (3)	Active II $R=3\times10^{-12}$ (4)	Active I saturation (5)	Active II saturation (6)	Semi-active damper I (7)	Semi-active damper II (8)	Passive ξ_{min} (9)	Passive ξ_{max} (10)
Control force	-	1048	1906	882	882	882	882	356	1306
Deck displacement	0.24	0.17	0.17	0.17	0.17	0.17	0.16	0.21	0.16
Isolator deformation	0.23	0.17	0.13	0.17	0.15	0.17	0.16	0.21	0.16
Column deformation	0.05	0.03	0.06	0.03	0.04	0.03	0.03	0.03	0.03
Column residual deformation	0.02	0.00	0.03	0.00	0.01	0.00	0.00	0.00	0.00

Table 2 Summary of peak control force and peak responses under Sun-Moon Lake record

Peak force (KN) and responses (m) (1)	Uncontrolled (2)	Active I $R=10^{-11}$ (3)	Active II $R=3\times10^{-12}$ (4)	Active I saturation (5)	Active II saturation (6)	Semi-active damper I (7)	Semi-active damper II (8)	Passive ξ_{min} (9)	Passive ξ_{max} (10)
Control force	-	1278	1947	882	882	882	882	468	1581
Deck displacement	0.54	0.35	0.37	0.36	0.37	0.36	0.36	0.47	0.40
Isolator deformation	0.41	0.26	0.18	0.28	0.27	0.29	0.29	0.38	0.27
Column deformation	0.25	0.13	0.25	0.12	0.12	0.11	0.10	0.17	0.14
Column residual deformation	0.11	0.09	0.20	0.04	0.07	0.03	0.04	0.04	0.11

columns and the isolators are perfect elastoplastic and bilinear elastoplastic, respectively. The parameters in Equations (1) and (2) are k_c =112.7 MN/m, α_c =0, x_{yc} =0.0309 m, A_c =1, $\beta_c=\gamma_c$ =0.5 and n_c =95 for the column, and k_b =47.6 MN/m, α_b =0.1912, x_{yb} =0.016 m, A_b =1, $\beta_b=\gamma_b$ =0.5 and n_b =95 for the isolators. The first and second natural periods of the isolated bridge with the initial elastic stiffness are 0.86 sec and 0.24 sec, respectively. The damping ratios of the system are assumed 2% for both modes. In simulation, the isolated bridge is subjected to two near-field ground motions recorded at JMA Kobe Observatory in the 1995 Kobe, Japan earthquake and Sun-Moon Lake in the 1999 Chi-Chi, Taiwan earthquake, as shown in Fig. 3.

In the uncontrolled system, the peak responses are presented in column 2 of Tables 1 and 2 under JMA Kobe record and Sun-Moon Lake, respectively. It is observed that the peak deck displacement reaches 0.54 m under Sun-Moon Lake ground motion and that the column has a residual displacement of 0.11 m, which results in the same magnitude of residual displacement in the deck.

(2) LQR optimum active control

With an actuator exerting the active control force by LQR optimum control algorithm, weighting matrix $\mathbf{Q}$ and R in Equation (7) have to be properly selected. A thorough parametric study showed that choosing $\mathbf{Q}$ as $diag[1,10^3,1,1]$ with off-diagonal elements to be zero achieves better performance in reducing the deck displacement. Larger weighting R results in smaller control force. The displacement responses under active controls with $R=10^{-11}$ and $R=3\times10^{-12}$ are presented in columns 3 and 4, respectively, of Tables 1 and 2. Both $R=10^{-11}$ and $R=3\times10^{-12}$ are effective in reducing the deck displacement, but larger control force does not achieve further decrease in deck displacement, even causes almost the same column deformation as the uncontrolled system and larger control residual displacement than the uncontrolled system.

Figure 4 compares the peak normalized deck displacement J_d with respect to the peak normalized control force J_U between the active control with $\mathbf{Q}$ as $diag[1,10^3,1,1]$ and R varying from 10^{-9} to 10^{-13}, and the passive control with damping coefficient varying from 0 kN/m/s to 8000 kN/m/s. J_d and J_U are defined as

$$J_d \equiv \max_t \|u_d(t)\| \Big/ \max_t \|\hat{u}_d(t)\| \tag{16}$$

$$J_U \equiv \max_t \|U(t)\| \Big/ W_{deck} \tag{17}$$

in which $u_d(t)$ and $\hat{u}_d(t)$ are the deck displacements in the controlled and uncontrolled

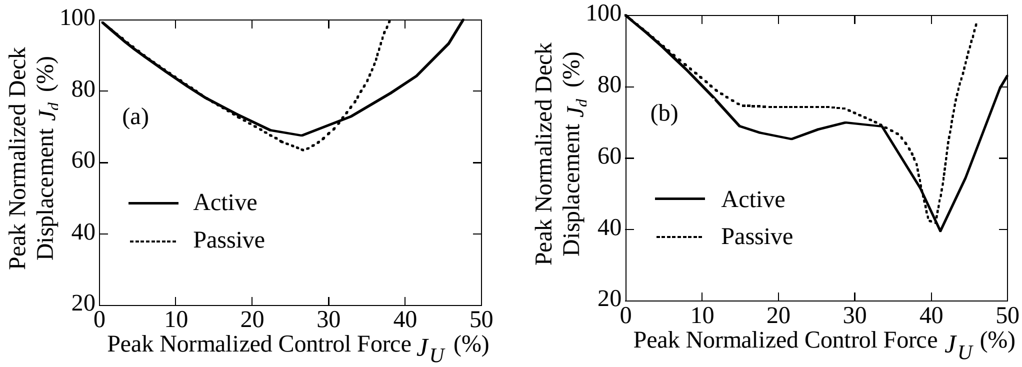

Figure 4 Comparison of peak normalized deck displacement between active control and passive control subjected to: (a) JMA Kobe, and (b) Sun-Moon Lake.

systems, respectively; $U(t)$ is the control force, and W_{deck} is the deck weight.

It is observed that the peak deck displacement decreases as the peak control force increases at smaller control force, namely $J_U \leq 27\%$ under JMA Kobe record and $J_U \leq 20\%$ under Sun-Moon Lake record. However, the peak deck displacement does not decrease monotonically, even increase, as the peak control force increases at larger control force. It can be attributed to that larger control force is effective for reducing isolator deformation while it also transfers larger force from the deck to the column so that it increases the column deformation. Once the increase of the column post-yield deformation surpasses the decrease of the isolator deformation, larger control force inversely increases the deck displacement. Moreover, the passive control shows close performance to the active control under JMA Kobe record for smaller peak control force, while the passive control are less effective than the active control under Sun-Moon Lake record.

Saturation of control force is thus used to avoid large column post-yield deformation. The displacement responses under active controls $R = 10^{-11}$ and $R = 3 \times 10^{-12}$ with saturation of the control force of 15% deck weight (882 kN) are presented in columns 5 and 6, respectively, of Tables 1 and 2. It is observed that the deck displacement decreases by almost the same as that of the unsaturated control and that the column residual displacement significantly decreases.

(3) Semi-active control

Variable viscous damper based on the LQR control algorithm is used to apply control force to the isolated bridge. The upper and lower bound of viscous coefficients of a variable damper, $\xi_{\max}$ and $\xi_{\min}$ in Equation (12), are 1000 kN/m/s and 250 kN/m/s, respectively. Fig. 5 compares the control force and the deck displacement response of the isolated bridge among uncontrolled, active controlled and semi-active controlled system, and shows the damping coefficient of variable viscous damper under Sun-Moon Lake ground motion. Weighting parameters in Equation (7) were assumed as $\mathbf{Q} = diag\ [1, 10^3, 1, 1]$ and $R = 10^{-11}$ and the saturation of control force was 15% deck weight under both active and semi-active control. As observed from Fig. 5, the control force by an actuator and a variable viscous damper is virtually the same except at few time periods. The force difference between two devices can be attributed to two reasons. One is that variable viscous dampers are intrinsically energy dissipation devices and cannot add energy to the structural system while actuators can generate arbitrary force no matter how the control force provides energy. The other reason is that the damping coefficient of variable viscous dampers is bounded. Although there is slight discrepancy, the semi-active control achieves similar performance to the active control. Under semi-active control, the peak deck displacement of the bridge reduces to 0.36 m and the residual displacement reduces to 0.03 m, which are almost the same as those under active control.

The hysteretic loops of the isolator and the column are shown in Fig. 6. These show that the column yields even under controlled systems and that both active and semi-active control have the similar hysteretic behavior. Figure 7 presents the hysteretic loops of control force and corresponding stroke. The hysteretic loops of active and semi-active control are similar. The force versus relative velocity for the control devices are shown in Fig. 8. These show that the damping coefficient of the variable viscous damper is confined, and that the actuator adds energy into system at $U(t)\dot{x}_b(t) < 0$.

Tables 1 and 2 present the peak responses of semi-active control in the columns 7 and 8. It is seen that semi-active control achieves slightly better

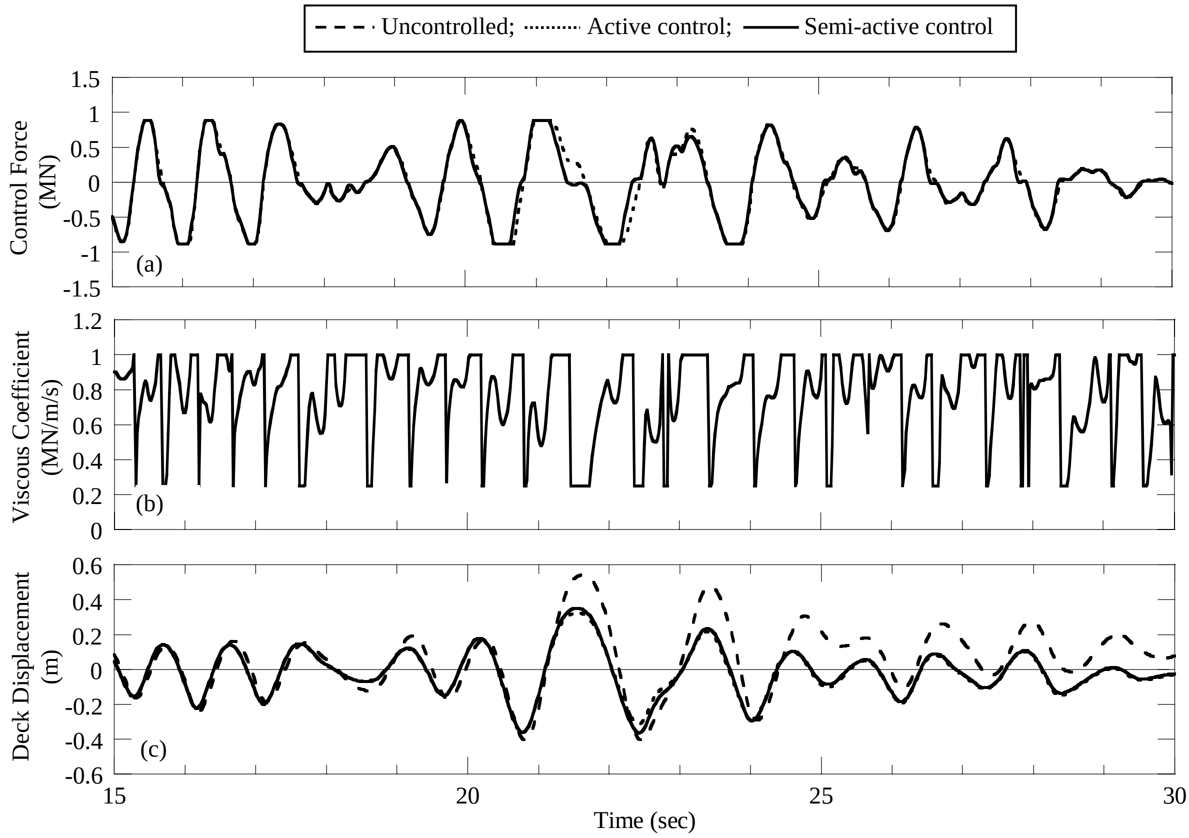

Figure 5 Comparison of the control force and the deck displacement (a) control force, (b) viscous coefficient of variable viscous damper, and (c) deck displacement.

performance than or similar performance to the active control under both ground motions. Furthermore, when the damping coefficient of the variable viscous damper is fixed at the minimum and maximum value, $\xi_{\min}$ and $\xi_{\max}$, the control effects are shown in the columns 9 and 10 of Tables 1 and 2. The results indicate semi-active control shows similar or slightly better performance than passive control with the maximum damping coefficient $\xi_{\max}$ of the variable viscous damper.

5. CONCLUSIONS

The application and effectiveness of semi-active control for nonlinear isolated bridge, which exhibits inelastic response at both the column and the isolator, was studied. The LQR control algorithm was used to command variable viscous dampers. Numerical simulations were carried out to investigate and compare the control performance of a five-span continuous highway elevated bridge under active, semi-active and passive control. The results indicate that semi-active control using variable viscous dampers is effective in reducing the deck displacement response and provides the similar performance by LQR active control using actuators. Semi-active control also shows similar or slightly better performance than passive control with the maximum damping coefficient $\xi_{\max}$ of the variable viscous damper.

ACKNOWLEDGMENT: The authors acknowledge support for the first author from the Center for Urban Earthquake Engineering (CUEE) in Tokyo Institute of Technology.

REFERENCES

1) Priestley, M. J. N., Seible, F. and Calvi, G. M.: *Seismic Design and Retrofit of Bridges*, John Wiley & Sons, USA, 1996.

2) Kawashima, K. and Unjoh, S.: Seismic response control of bridges by variable dampers, *Journal of Structural Engineering*, American Society of Civil Engineers, **120(9)**, 2583-2601, 1994.

3) Yang, J. N., Wu, J.C., Kawashima, K. and Unjoh, S.: Hybrid control of seismic-excited bridge structures, *Earthquake Engineering and Structural Dynamics*, **24(11)**, 1437-1451, 1995.

4) Symans, M. D., Kelly, S.W.: Fuzzy logic control of bridge structures using intelligent semi-active seismic isolation systems, *Earthquake Engineering and Structural Dynamics*, **28(1)**, 37-60, 1999.

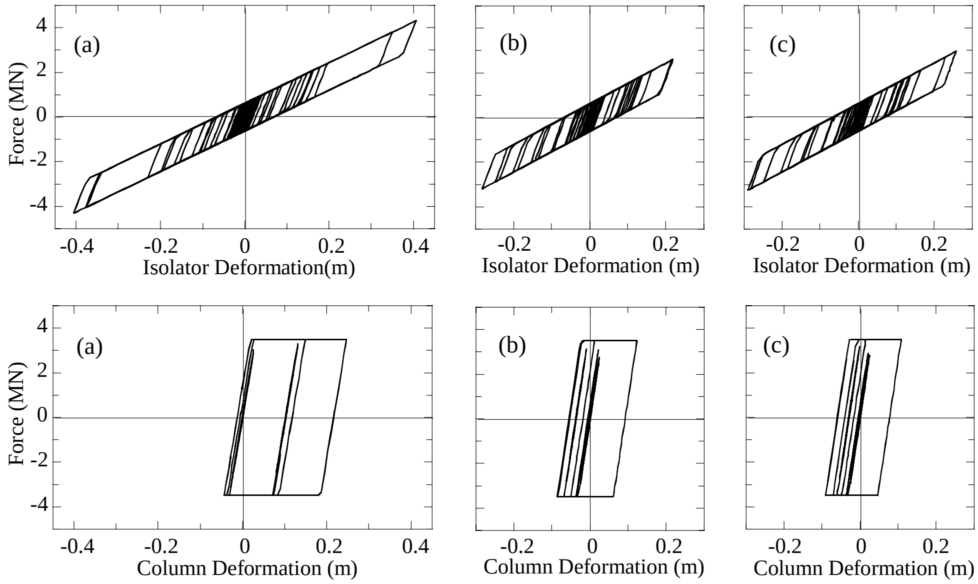

Figure 6 Hysteretic loops of the isolator and the column: (a) uncontrolled, (b) active control, and (c) semi-active control.

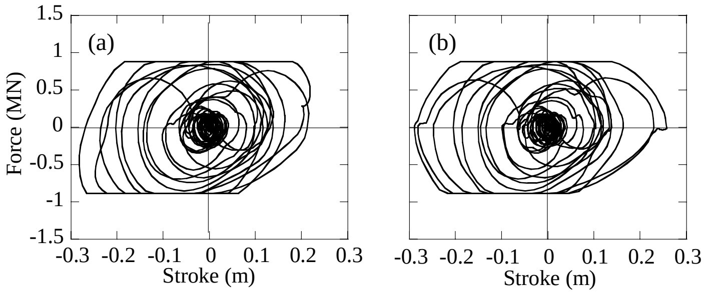

Figure 7 Hysteretic loops: (a) actuator, and (b) variable viscous damper

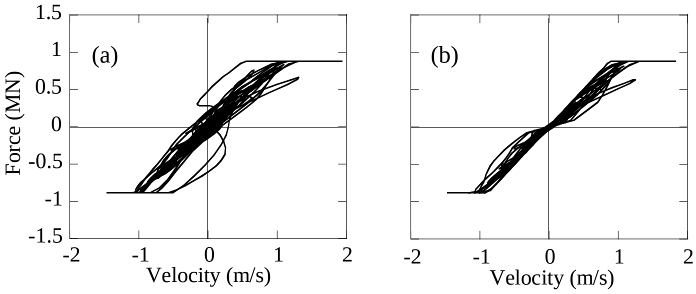

Figure 8 Control force vs. velocity: (a) actuator, and (b) variable viscous damper

5) Loh, C. H., Wu, L. Y. and Lin, P. Y.: Displacement control of isolated structures with semi-active control devices, *Journal of Structural Control*, **10**, 77-100, 2003.

6) Symans, M. D. and Constantinou, M. C.: Seismic testing of a building structure with a semi-active fluid damper control system, *Earthquake Engineering and Structural Dynamics*, **26(7)**, 759-777, 1997.

7) Yang, J. N., Li, Z. and Vongchavalitkul, S.: A generalization of optimal control theory: linear and nonlinear control, *National Center for Earthquake Engineering Research Technical Report*, NCEER-92-0026, USA, 1992.

8) Yang, J. N., Li, Z. and Vongchavallitkul, S.: A generalization of optimal control theory: linear and nonlinear control, *Journal of Engineering Mechanics*, American Society of Civil Engineers, **120(2)**, 266-283, 1994.

9) Wen, Y. K.: Method for random vibration of hysteretic system, *Journal of Engineering Mechanics Division*, American Society of Civil Engineers, **102(EM2)**, 249-263, 1976.

10) Soong, T. T.: *Active Structural Control: Theory and Practice*, Longman, UK, 1990.

11) Japan Road Association: *Design specification of highway bridges, part V seismic design,* Tokyo: Maruzen, 1996.

(Received March 15, 2005)